Insect Swarms and Chemoattractants

Andy Leverentz
Harvey Mudd College
Math 164: Scientific Computing

May 2, 2007

1 Introduction

The study of biological swarming is an emerging area of research in applied mathematics. Models that describe the aggregate behavior of swarms in terms of individual interactions may be useful both for biologists investigating the connection between localized interaction mechanisms and larger-scale swarming phenomena, and also for engineers attempting to emulate natural swarm behavior in artificial swarms. Previous papers have studied the effect of particular types of pairwise interaction forces on swarm-wide behavior (see, for example, [1] and [2]).

In this paper, we consider a one-dimensional swarm of insects governed by a simple mechanism involving chemoattraction in addition to pairwise interactions. We suppose that the insects are influenced by only two types of forces: (1) attraction to a fixed, external source of chemoattractant, and (2) social repulsion. Both a discrete and a continuous model are proposed to describe the motion of these swarms, with the hypothesis that the behavior of the discrete model approaches that of the continuous model as the number of insects increases. Finally, numerical simulations of each model are used to test this hypothesis.

2 The Discrete Model

For a discrete swarm containing N individuals, let $x_1, x_2, \ldots, x_N \in \mathbb{R}$ denote the position of each insect. If we assume that each insect is influenced only by chemoattraction and social repulsion, the governing equations for this system are given by

$$\frac{dx_i}{dt} = F_c(x_i) + \sum_{j \neq i} m_i F_s(x_i - x_j).$$

Here, F_c and F_s are functions describing the chemoattractive and social repulsive forces, respectively, and m_i is a measure of the "social mass" (i.e., the degree of repulsive influence) of the ith insect. All quantities have been non-dimensionalized in this model, as well as in the continuous model below.

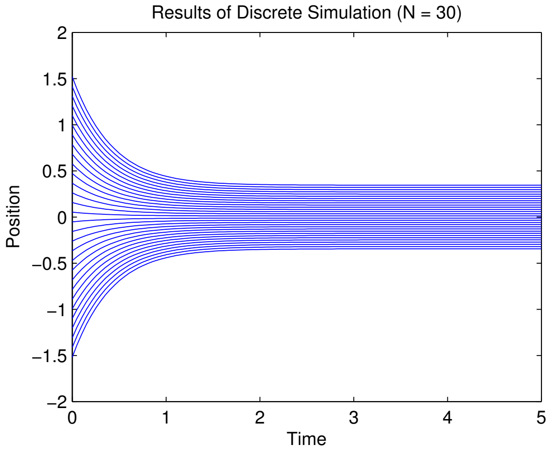

Figure 1: Results of Discrete Simulation. For this simulation, the swarm size was set to $N = 30$.

The governing equations above constitute a system of first-order ODEs, making them straightforward to solve numerically. Matlab's built-in ODE solver `ode45`, which implements an adaptive 4th-order Runge-Kutta scheme, was used to simulate this model. For the purposes of this simulation, a social mass of $m_i = 1/N$ was used for each insect in order to guarantee a total social mass of 1 regardless of the number of individuals. Moreover, the chemoattractive force was taken to be

$$F_c(x) = -\frac{d}{dx}\left(x^2\right) = -2x,$$

with a social repulsive force given by

$$F_s(r) = -\frac{d}{dr}(e^{-|r|}) = \text{sign}(r) \cdot e^{-|r|}.$$

Note that these forces can be interpreted as gradients of potential functions.

Initial tests of this simulation suggested that the eventual steady state of the system was independent of initial conditions. Figure 1 shows the result of a typical simulation run.

3 The Continuous Model

3.1 Equation of Motion

In the continuous model, the distribution of insects in a swarm is described by a continuous density function $\rho(x, t)$. We expect social mass to be conserved in this system, so we use the following conservation law as the equation of motion:

$$\frac{\partial \rho}{\partial t} + \frac{\partial}{\partial x}(v\rho) = 0. \tag{1}$$

Here, the velocity v of the swarm at each point is given by

$$v(x, t) = F_c(x) + \int_{\mathbb{R}} \rho(z, t) F_s(x - z)\, dz,$$

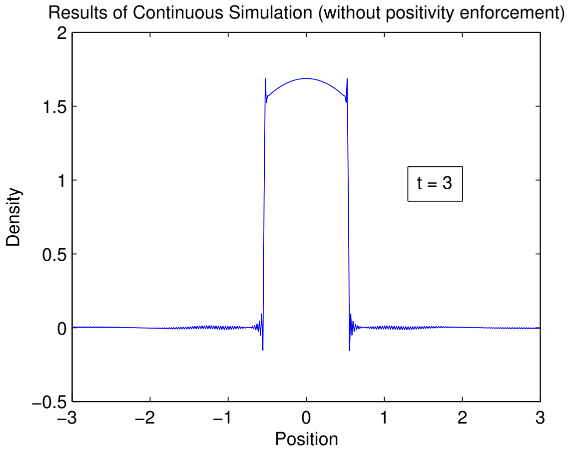

Figure 2: Results of Continuous Simulation, Without Positivity Enforcement. Note that oscillations occur near the edge of the swarm and extend into the region where we expect the swarm density to be identically zero. This effect is likely the result of finite differences being used on a function that has a jump discontinuity, although later tests indicate that the oscillations can be significantly reduced simply by disallowing negative swarm densities.

and the functions F_c and F_s once again describe the chemoattractive and social repulsive forces. Note that v can be interpreted as the continuous analogue of dx_i/dt from the discrete case, with the sum being replaced by an integral.

3.2 Numerical Approach and Simulation Results

To implement a numerical simulation of this model, the spatial domain must be limited to a finite interval $-L \leq x \leq L$ and then discretized, yielding a finite set $x_1, \ldots, x_N$ of spatial coordinates. Given an initial condition, we know $\rho(x_i, t_0)$ for all i. Thus, we can estimate $v(x_i, t_0)$ using quadrature (specifically, the trapezoid rule, in the present implementation) to compute an approximation to the integral expression. Knowing $v(x_i, t_0)$ and $\rho(x_i, t_0)$, we can then estimate the spatial derivative of the flux $v\rho$ at every grid point. This is accomplished using second-order centered difference formulas. To compute this derivative at the endpoints of the simulation domain, the boundary condition $\rho(x, t) = 0$ is enforced for $x = \pm L$. Then, using Eq. (1), we have an approximation for $\partial\rho/\partial t$, which in turn allows us to estimate ρ at $t = t_0 + \Delta t$. Repeating this process for each time step, we obtain an approximate solution to Eq. (1). Forward-stepping in time was initially implemented using Euler's method, although this required prohibitively small time steps to ensure numerical stability. Consequently, the current implementation uses a non-adaptive 4th-order Runge-Kutta scheme to achieve well-behaved solutions with fewer time steps.

Preliminary tests revealed several problems with this implementation. Regardless of initial conditions, the numerical solution appeared to develop a jump discontinuity at the edge of the swarm (ie, at the endpoints of the spatial interval on which $\rho > 0$). Near this steep gradient, the solution developed oscillations, causing the swarm density ρ to become negative at several points. This behavior is illustrated in Figure 2.

To resolve this issue, the simulation was modified to guarantee non-negative solutions.

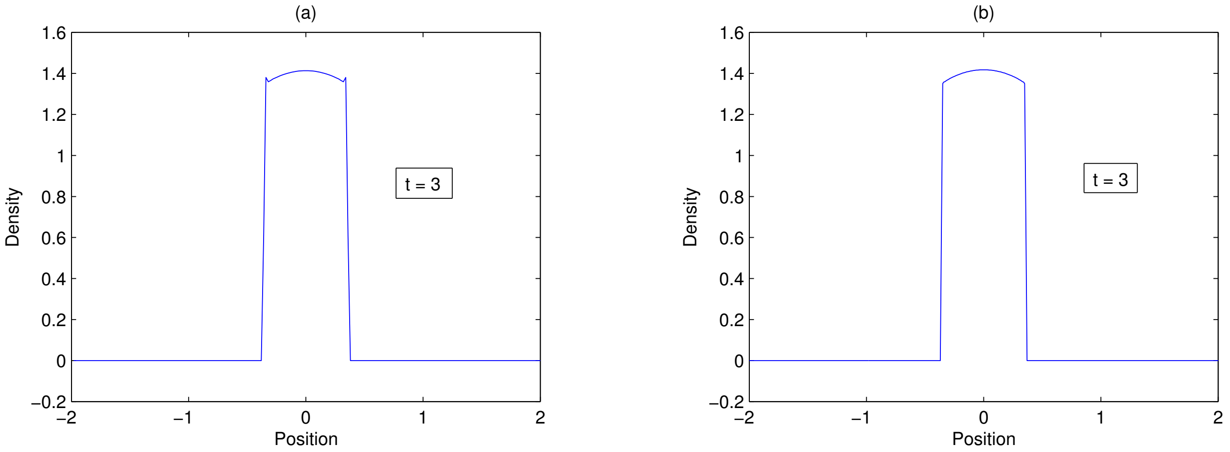

Figure 3: Results of Continuous Simulation, With Positivity Enforcement. In (a), we see that the inclusion of positivity-enforcement reduces the presence of oscillations. In (b), the combination of positivity-enforcement and a finer spatial grid eliminates the oscillations almost entirely.

At each time step, ρ is set to zero wherever it has become negative. Then, because the elimination of negative density effectively adds mass to the system, conservation of mass must also be explicitly enforced. This is accomplished by adjusting the mass of the system at each time step to match the system's initial mass. This modification eliminates most (but not all) of the undesired oscillations, as can be seen in Figure 3.a. Subsequent refinement of the spatial grid eliminates these oscillations almost entirely (see Figure 3.b).

As with the discrete case, the choice of initial conditions appears to have no noticeable impact on the asymptotic steady-state behavior of the system. Figure 4 shows a typical run of the simulation, using an isolated cosine bump as the initial condition.

4 Comparing the Two Models

By comparing Figures 1 and 4, we see that the two models yield qualitatively similar behavior. However, there is some difficulty in comparing the results quantitatively. In the discrete case, the simulation produces a list of x-coordinates at which insects can be found, whereas the continuous simulation yields a real-valued density function sampled at points on a fixed spatial grid.

At a given time t, we can think of the discrete simulation as producing a density function consisting of finitely many superimposed Dirac δ-functions, which represent concentrated point-masses. Under this interpretation, we can define a cumulative mass function

$$P_t(x) = \int_{-\infty}^{x} \rho(z,t)\,dz,$$

which makes sense in both the discrete and the continuous model. We can quantitatively measure the degree to which the results differ by comparing the cumulative mass functions resulting from the two simulations. In order to obtain results that have a more direct

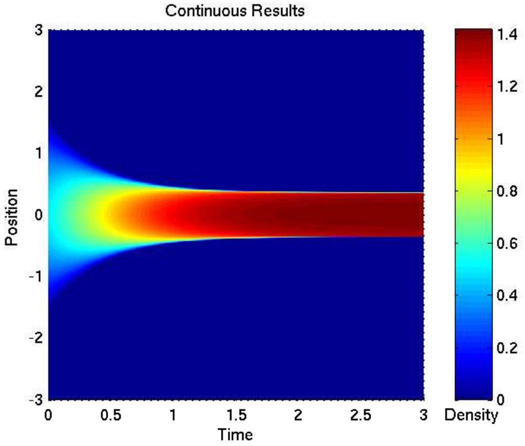

Figure 4: Results of Continuous Simulation (density vs. position and time). Note the qualitative similarity between the continuous results shown here and the discrete results shown in Figure 1.

physical interpretation, however, we can additionally construct a continuous approximation to the discrete density function. This is accomplished by fitting interpolating polynomials to the cumulative density function $P_t(x)$, and then differentiating these polynomials at each point of discontinuity. We can interpret these results as values sampled from a continuous function which approximates a discrete density function. These sampled density values can then be compared directly to the results of the continuous simulation. Figures 5 and 6 show the results of such a comparison.

To test the hypothesis that the behavior of the discrete model approaches that of the continuous model in the limit of large N, the discrete simulation was run several times with successively larger swarm sizes. Additionally, the continuous simulation was run on successively finer spatial grids to obtain a better approximation to the continuous equilibrium distribution. The results of these tests suggest that the discrete results are converging to a single continuous density function (see Figure 5). Moreover, there is a discrepancy of less than 1% between the most refined discrete results and the most refined continuous results (see Figure 6). Therefore, it seems reasonable to conclude that our hypothesis is correct.

5 Future Work

The most significant shortcoming of the current simulation is that positivity and mass-conservation must be enforced explicitly at each time step. It is possible that these adjustments may reduce the faithfulness of the simulation to the original model. In place of the current implementation, it would be ideal to have a numerical scheme capable of preserving positivity and conserving mass without corrections at each time step.

Moreover, for the purposes of studying this model with a different set of forces, it would be helpful, especially in the continuous case, to increase the accuracy of the numerical scheme without significantly reducing its efficiency. This might be accomplished by using higher-order finite difference formulas and quadrature methods, or perhaps by switching to an

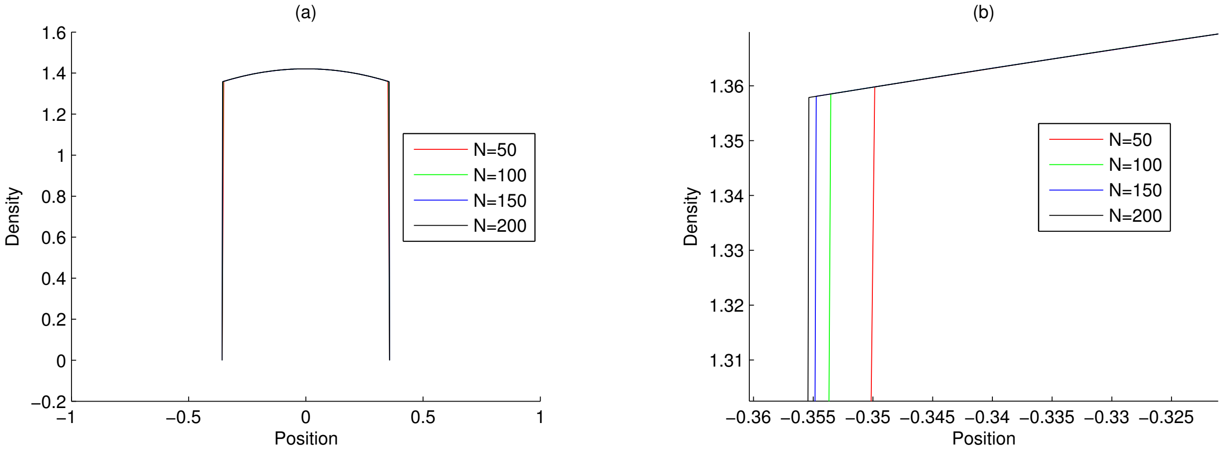

Figure 5: Continuous Approximations to Discrete Density. In (a), we see the results of fitting continuous density approximations to the steady-state positions of discrete swarms for several different values of N. The plot in (b) is a magnified version of the same results, centered on the discontinuity occuring at the edge of the swarm. These results suggest that the density approximations are converging to a single continuous distribution as the number of insects N increases.

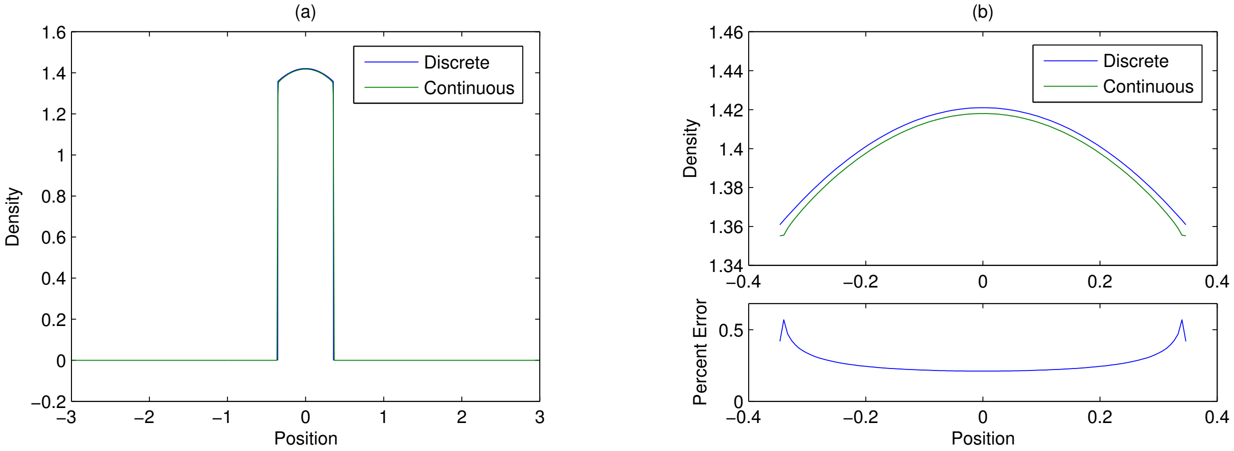

Figure 6: Discrete vs. Continuous Results. In plot (a), the curve labeled “continuous” is the result of running the continuous simulation to equilibrium. The curve labeled “discrete” is the result of running a discrete simulation to equilibrium and then fitting a continuous density approximation to the resulting steady-state positions. In the continuous case, the simulation used 900 spatial grid points; for comparison, the discrete simulation was run with a swarm size of $N = 200$. Plot (b) shows a closer view of the same results. The discrepancy between the two distributions remains less than 1% wherever the swarm densities are nonzero.

implicit numerical method.

It may also be interesting to study the steady-state behavior of these models by solving for the equilibrium distributions directly (that is, by solving the equations of motion when $\partial\rho/\partial t$ or dx_i/dt is set to zero). Even if this is not a tractable problem analytically, it may be worthwhile to attempt to find the steady states numerically.

Furthermore, now that we have seen evidence suggesting that the behavior of the discrete model approaches that of the continuous model in the limit of large N, it seems reasonable to attempt to prove this analytically.

Acknowledgments

I would like to thank Professors Andrew Bernoff (HMC), Darryl Yong (HMC), and Chad Topaz (USC) for patiently guiding me through the development of these models and simulations.

References

[1] A. Mogilner et al., *Mutual interactions, potentials, and individual distance in a social aggregation*, Journal of Mathematical Biology, 47 (2003) pp. 353-389.

[2] M.R. D'Orsogna et al., *Self-Propelled Particles with Soft-Core Interactions: Patterns, Stability, and Collapse*, Physical Review Letters, 96, 104302 (17 March 2006) pp. 1-4.